Volume 261, Issues 3–4 30 September 2007 ISSN 0012-821X

ELSEVIER

EARTH & PLANETARY SCIENCE LETTERS

Available online at www.sciencedirect.com
ScienceDirect
Earth and Planetary Science Letters 261 (2007) 551–564
EPSL
www.elsevier.com/locate/epsl

Supercontinent cycles, true polar wander, and very long-wavelength mantle convection

Shijie Zhong [a,*], Nan Zhang [a], Zheng-Xiang Li [b], James H. Roberts [c]

[a] Department of Physics, University of Colorado, Boulder, Colorado 80309, USA
[b] Dept. of Applied Geology, Curtin University of Technology, GPO Box U1987, Perth, WA 6845, Australia
[c] Department of Earth and Planetary Sciences, University of California at Santa Cruz, Santa Cruz, California 95064, USA

Received 2 April 2007; received in revised form 11 July 2007; accepted 13 July 2007
Available online 3 August 2007
Editor: R.D. van der Hilst

Abstract

We show in this paper that mobile-lid mantle convection in a three-dimensional spherical shell with observationally constrained mantle viscosity structure, and realistic convective vigor and internal heating rate is characterized by either a spherical harmonic degree-1 planform with a major upwelling in one hemisphere and a major downwelling in the other hemisphere when continents are absent, or a degree-2 planform with two antipodal major upwellings when a supercontinent is present. We propose that due to modulation of continents, these two modes of mantle convection alternate within the Earth's mantle, causing the cyclic processes of assembly and breakup of supercontinents including Rodinia and Pangea in the last 1 Ga. Our model suggests that the largely degree-2 structure for the present-day mantle with the Africa and Pacific antipodal superplumes, is a natural consequence of this dynamic process of very long-wavelength mantle convection interacting with supercontinent Pangea. Our model explains the basic features of true polar wander (TPW) events for Rodinia and Pangea including their equatorial locations and large variability of TPW inferred from paleomagnetic studies. Our model also suggests that TPW is expected to be more variable and large during supercontinent assembly, but small after a supercontinent acquires its equatorial location and during its subsequent dispersal.

Keywords: mantle convection; supercontinents; true polar wander; superplumes

1. Introduction

The Earth's large-scale continental tectonics for the last 1 Ga including mountain building, volcanism and rifting are predominated by the cyclic processes of assembly and breakup of supercontinents Rodinia (Hoffman, 1991; Torsvik, 2003; Dalziel, 1991; Moores, 1991; Li et al., 2004; Li et al., in press) and Pangea (Hoffman, 1991; Smith et al., 1981; Scotese, 1997). The primary assembly of Pangea occurred ~330 Ma ago in the Carboniferous as Gondwana and Laurussia collided near the equator (Hoffman, 1991; Smith et al., 1981; Scotese, 1997) (Fig. 1a). The formation of Pangea and the collisions among continental blocks generated mountain belts including Appalachians and Urals. The breakup of Pangea started ~175 Ma ago during the Middle Jurassic, first with North America breaking away from Africa, South America and Eurasia, followed with a sequence of breakups from ~140 Ma to 100 Ma in the Cretaceous between Antarctic, Australia, Africa and South America (Hoffman, 1991; Smith et al., 1981; Scotese, 1997). The

* Corresponding author.
E-mail address: szhong@colorado.edu (S. Zhong).

0012-821X/$ - see front matter © 2007 Elsevier B.V. All rights reserved.
doi:10.1016/j.epsl.2007.07.049

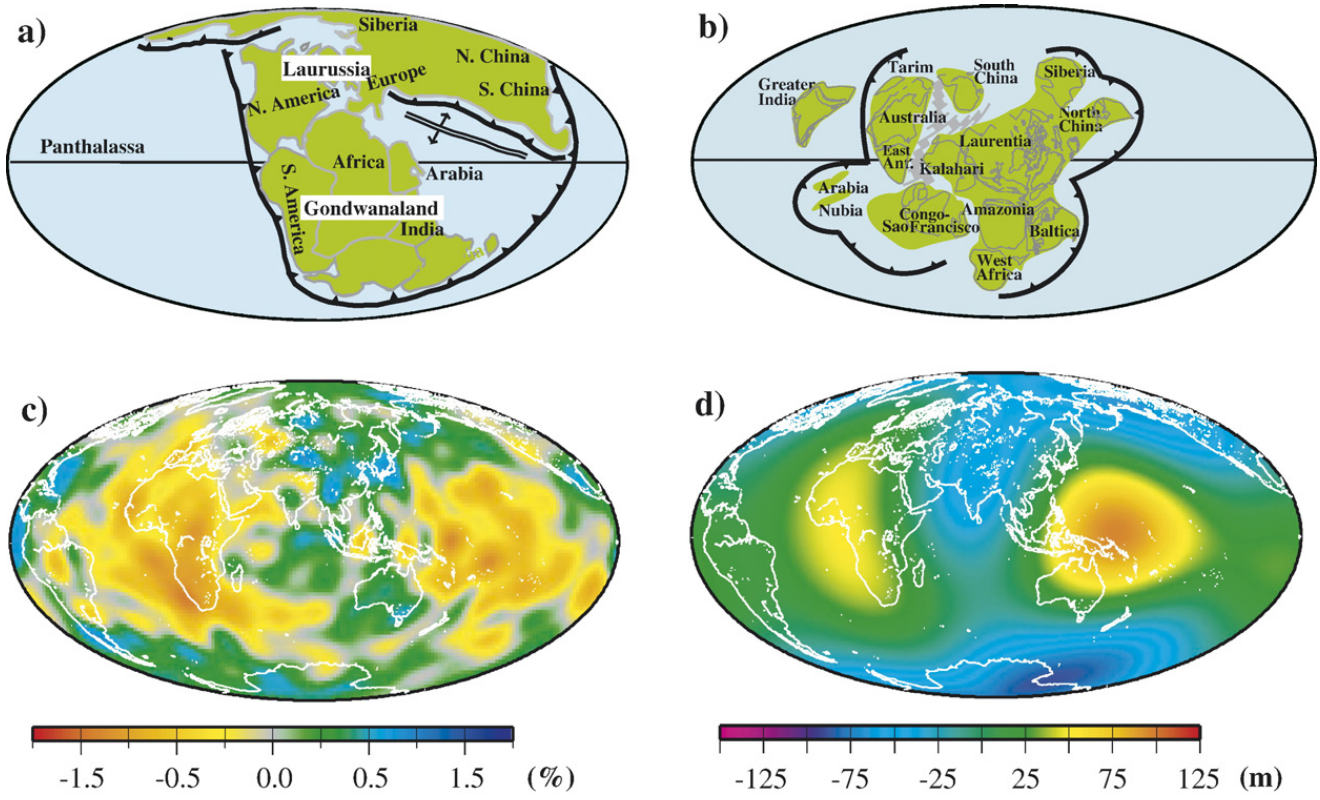

Fig. 1. Reconstruction of supercontinents Pangea at 195 million years ago (Scotese, 1997) (a) and Rodinia at 750 million years ago (Li et al., in press) (b) shortly before their breakup, seismic structure for present-day mantle above the core–mantle boundary (Ritsema et al., 1999) (c), and the long-wavelength geoid anomalies (degrees 2 and 3 only) (d).

assembly of Rodinia nucleated around Laurentia and was responsible for a large number of mountain belts including the Grenville orogen (1.3 Ga–1 Ga) (Hoffman, 1991; Torsvik, 2003; Dalziel, 1991; Moores, 1991; Li et al., 2004; Li et al., in press) (Fig. 1b). By ~900 Ma ago, the assembly of Rodinia was largely complete. The breakup of Rodinia may have started ~750 Ma ago, as India, Australia–East Antarctica, and South China broke away from Laurentia (Li et al., in press). Some of those continental blocks that broke away from Laurentia may have eventually merged to form Gondwana by 540–530 Ma (Hoffman, 1991).

Supercontinent processes have implications for the structure and dynamics of the mantle. Both Rodinia and Pangea were largely surrounded by subduction zones (Figs. 1a and b). This leads to kinematic models suggesting that supercontinent cycles require mantle convection of very long-wavelengths at spherical harmonic degree 1 (i.e., one hemisphere with downwellings and the other hemisphere with upwellings) or degree 2 (i.e., two antipodal upwellings) (Monin, 1991; Evans, 2003). The present-day mantle is predominated by degree-2 structures that include the circum-Pacific seismically fast, cold anomalies and two large seismically slow, hot anomalies beneath Africa and Pacific (Dziewonski, 1984; Masters et al., 2000; Ritsema et al., 1999; Romanowicz and Gung, 2002; Van der Hilst, 1997; Grand, 2002) (Fig. 1c). These seismically derived long-wavelength mantle structures are closely related to plate motion history in the last 120 Ma (Lithgow-Bertelloni and Richards, 1998; Ricard et al., 1993; Bunge et al., 1998; McNamara and Zhong, 2005a) that can be reconstructed based on seafloor observations (Lithgow-Bertelloni and Richards, 1998). Isochemical mantle convection (Lithgow-Bertelloni and Richards, 1998; Bunge et al., 1998) with the 120 Ma plate motion history reproduces the distribution of subducted slabs in the mantle. Dynamic interaction between the plate motion history and a thin, chemically distinct and dense layer above the core–mantle boundary (CMB) (McNamara and Zhong, 2005a) further explains the distribution of African and Pacific seismically slow anomalies. However, beyond 120 Ma except for continents, global plate motion history is not well constrained by seafloor observations. Nevertheless, it is reasonable to assume that the plate motion history since the Pangea time is dictated by the breakup of Pangea that may continue to influence the present-day mantle structures.

Supercontinent cycles may also be related to true polar wander (TPW) (Evans, 2003; Anderson, 1982; Li et al., 2004). TPW is controlled by the degree-2 components of

the geoid (Goldreich and Toomre, 1969; Steinberger and O'Connell, 1997; Richards et al., 1997) and is indicative of structure change of mantle convection. Anderson (1982) suggested that the Pangea's equatorial location (Fig. 1a) resulted from two antipodal geoid highs above Africa and the central Pacific (Fig. 1d) that were caused by Pangea's thermal insulation effects. However, while Pangea was centered near the present-day Africa, the proposed insulation at the central Pacific is inconsistent with the configuration of Pangea (Fig. 1a) (Hoffman, 1991; Smith et al., 1981; Scotese, 1997). Also, Pangea does not seem to experience significant TPW after Gondwana and Laurussia collided near the equator to form Pangea ~250 Ma ago (Evans, 2003). However, recent paleomagnetic studies indicate significant TPW for Rodinia before its breakup (Li et al., 2004; Li et al., in press; Maloof et al., 2006).

Surface plate motion including supercontinent cycles is undoubtedly controlled by mantle convection. Based on two-dimensional models of mantle convection, Gurnis (1988) suggested that continents collide to form a supercontinent above downwellings and that the supercontinent may subsequently be dispersed by upwellings that develop below the supercontinent. However, the three-dimensional planform of mantle convection, a likely important factor for supercontinent cycles (Monin, 1991; Evans, 2003), has not been investigated in relevant dynamic models, although a number of studies have examined the effects of supercontinents on the dynamics and structure of the mantle (Zhong and Gurnis, 1993; Lowman and Jarvis, 1996; Lowman and Jarvis, 1995; Phillips and Bunge, 2005). A mantle convection planform characterized by short-wavelength structures with a large number of downwellings may not lead to supercontinent assembly, because continental blocks may be trapped by different downwellings and hence do not collide together. Therefore, long-wavelength mantle convection may be necessary for supercontinent assembly (Monin, 1991; Evans, 2003). Particularly, a spherical harmonic degree-1 planform with all the downwellings in one hemisphere and upwellings in the other hemisphere would inevitably lead to supercontinent assembly (Monin, 1991; Zhong and Zuber, 2001).

Radially stratified mantle viscosity may greatly affect the planform of mantle convection (Zhong and Zuber, 2001; Jaupart and Parsons, 1985; Bunge et al., 1996; Tackley, 1996; Lenardic et al., 2005; Zhang and Yuen, 1995). Bunge et al. (1996) showed, using three-dimensional spherical shell convection models with only depth-dependent viscosity, that a viscosity increase from the upper to lower mantles by a factor of 30, as constrained by the geoid observations (Hager and Richards, 1989), leads to increased wavelengths for mantle structures that are predominated at degree-6. In attempting to understand the origin of globally asymmetric structures for other planetary bodies including the Martian crustal dichotomy and lunar mare basalts, models of stagnant-lid mantle convection have demonstrated that mantle convection with a degree-1 planform can be obtained with a sufficiently weak asthenosphere (Zhong and Zuber, 2001; Parmentier et al., 2002; Roberts and Zhong, 2006). A degree-1 planform can also be obtained with a moderately strong lithosphere and without a weak asthenosphere for Earth-like mobile-lid convection (McNamara and Zhong, 2005b; Harder, 2000; Yoshida and Kageyama, 2005), but only under moderate convective vigor or Rayleigh number (McNamara and Zhong, 2005b).

There are two objectives in this study. The first is to examine the effects of temperature-dependent viscosity, lithospheric viscosity and viscosity increase at 670-km depth on the planform of mantle convection, particularly the degree-1 planform, in mobile-lid convection. The second is to investigate the role of the planform of mantle convection in supercontinent cycles and their implications for time evolution of mantle structure, TPW, and the present-day Earth's mantle structure. The paper is organized as follows. First, the models and methods used are described in Section 2. Next, the model results on the planform of mantle convection and the associated TPW are presented in Section 3. Section 4 contains a discussion of the implications of our results for supercontinent cycles and TPW. Finally, our conclusions are summarized in Section 5.

2. Methods and models

This study uses three-dimensional spherical shell thermal convection models for an incompressible fluid with the Boussinesq approximation. The conservation equations of the mass, momentum, and energy and their non-dimensionalization schemes are described in Zhong et al. (2000). The nondimensional inner and outer radii are $r_b = 0.55$ and $r_t = 1$, respectively. The models include both the basal and internal heating, and constant material properties and thermodynamic constants except for mantle viscosity which is both depth- and temperature-dependent. Depth-dependent thermodynamic parameters (e.g., coefficient of thermal expansion and thermal conductivity) may affect convective planform (Zhang and Yuen, 1995), but their effects may not be as strong as the depth-dependent viscosity (Roberts and Zhong, 2006). Therefore, we focus the effects of depth-dependent viscosity in this study.

A linearized viscosity equation with a nondimensional form is used: $\eta = \eta_0(r)\exp[E(0.5 - T)]$, where T and E

are the temperature and activation energy, respectively, and the pre-exponential constant $\eta_0(r)$ reflects the depth-dependence. In this study, E is chosen to be 6.9078, which gives rise to a factor of 10^3 viscosity variation for temperature varying from 0 to 1 and mobile-lid convection with moderately strong lithosphere.

Two controlling non-dimensional parameters in our thermal convection models are internal heat generation rate γ and Rayleigh number Ra. Internal heat generation rate $\gamma = Hh^2/\kappa\Delta T$ and Rayleigh number $Ra = \rho g \alpha \Delta T h^3/\kappa\eta_r$, where H, ρ, κ, and α are the volumetric heat generation rate, density, thermal diffusivity, and coefficient of thermal expansion of the mantle, respectively, η_r is the reference viscosity and is the lower mantle viscosity at $T=0.5$, g is the gravitational acceleration, ΔT is the temperature difference across the mantle, and h is the mantle thickness. The models are computed on a numerical grid with either 1.4 million or 3.3 million nodes, depending on Ra. The calculations are done on a 48-processor PC-Cluster using a 3-D spherical convection code CitcomS (Zhong et al., 2000) which is modified from the Cartesian Citcom (Moresi and Gurnis, 1996).

Two types of models are computed, one with no continents and the other with a supercontinent. For models with no continents, free-slip and isothermal boundary conditions are applied at the surface and CMB. For cases with a supercontinent, velocity boundary conditions are applied differently at the supercontinent, while boundary conditions remain the same for CMB and outside of supercontinent. The supercontinent is modelled as a high viscosity, fixed disc that is 150 km thick and occupies 30% of the Earth's surface area. Surrounding the supercontinent is a 300 km wide weak zone that facilitates circum-supercontinent subduction (Gurnis, 1988; Zhong and Gurnis, 1993). The viscosity of the supercontinent is taken as 30 times larger than that of other parts of the surface, while the viscosity of the weak zone is reduced by a factor of 10 relative to the non-supercontinent surface (Gurnis, 1989; King and Hager, 1990), both of which are accomplished via varying the pre-exponential constant. This technique is similar to that used in Gurnis (1988) and Zhong and Gurnis (1993). More discussions on modelling the supercontinent will be presented later.

For models with no continents, initial temperature conditions consist of a radial temperature profile $T_0(r)$ superimposed with either random perturbations or perturbations at a given spherical harmonic degree l and order and m. $T_0(r)$ is 0.5 for the mantle interior and changes linearly to boundary temperatures 0 or 1 across the top and bottom thermal boundary layers, respectively. The magnitude of the perturbations is 0.01. As we will demonstrate later, our results for models with no continents do not depend on initial conditions. The initial temperature for models with a supercontinent is from corresponding models with no continents and will be discussed later.

The Earth's rotational stability is controlled by degree-2 geoid anomalies (Goldreich and Toomre, 1969). TPW occurs to place the negative long-wavelength geoid at the poles and the positive at the equator (Steinberger and O'Connell, 1997; Richards et al., 1997). TPW calculations are done for a number of representative cases to predict the rotational pole positions. The TPW calculations consist of three steps. 1) Using CitcomS and post-processing procedures (Zhong and Davies, 1999), the geoid is computed by considering the dynamic compensation effects (Hager and Richards, 1989). 2) The degree-2 components of the geoid are used to construct the moment of inertia tensor (Lambeck, 1980). 3) Determine pole positions by solving an eigen-value problem in diagonalizing the moment of inertia tensor. This procedure is used in Roberts and Zhong (2007) and is similar to that in Steinberger and O'Connell (1997). Relevant model parameters needed for computing the geoid are listed in Table 1, along with other parameters. While the magnitude of the geoid depends on the choice of the parameters, the pattern of the geoid and TPW calculations is independent of the model parameters.

3. Results

This section first presents results for planform of mantle convection in models with no continents, which is then followed with results on the effects of a supercontinent on the thermal structure. TPW calculations are then presented for models relevant to supercontinent cycles.

3.1. Planform of mantle convection in models with no continental block

Case 1 uses Rayleigh number $Ra = 4.56\times10^6$, internal heating $\gamma = 10.1$, and pre-exponential factor $\eta_0(r) = 1$ throughout the mantle (Table 2). The initial temperature

Table 1
Material properties

Parameters	Value
Earth's radius, R	6370 km
Mantle thickness, h	2866.5 km
Gravitational acceleration, g	9.8 $m\cdot s^{-2}$
Mantle density, ρ	3300 $kg\cdot m^{-3}$
Thermal diffusivity, κ	10^{-6} $m^2\cdot s^{-1}$
Coefficient of thermal expansion, α	3×10^{-5} K^{-1}
Temperature difference, ΔT	2500 K
Thermal conductivity, k	3.3 $W\ m^{-1}\ K^{-1}$

Table 2
Model parameters and output

Case [a]	Ra ($\times 10^6$)	γ	η_{0lith} [b]	η_{0um} [b]	I.C. (l,m) [c]	ξ (%) [d]	Q_s [d] (mW/m^2)	V_s [d] (cm/yr)	Structure [e]
1	4.56	10.1	1	1	(3,2)	50	48	0.5	l=6
2	4.56	10.1	1/30	1/30	(3,2)	44	53	1.5	l=8
3	4.56	10.1	1	1/30	(3,2)	40	44	3.1	(74,275)
4	4.56	10.1	1	1/30	Random	37	43	2.9	(84,68)
5	4.56	10.1	1	1/30	(6,4)	38	44	3.0	(−65,254)
6	4.56	26.3	1	1/30	(3,2)	61	56	3.4	(−83,353)
7	1.37	10.1	1	1/30	(3,2)	38	31	1.4	(25,131)
8	13.7	10.1	1	1/30	(3,2)	29	56	5.9	(26,283)
9	13.7	20.2	1	1/30	Random	42	64	6.1	(−0.2,132)
10	4.56	10.1	0.4	1/30	(3,2)	41	49	4.2	(36,282)
11	4.56	10.1	0.2	1/30	(3,2)	48	54	2.9	l=2,4
3A	4.56	10.1	1	1/30	Case 3	36	40	1.7	l=2

[a] Cases 8 and 9 with high Ra use 3.3 million nodes (i.e., 65 nodes in each dimension for each of the 12 caps using CitcomS discretization), while other cases use 1.1 million nodes (i.e., 49 nodes in each dimension for each cap). Grid refinement is applied in the top and bottom thermal boundary layers.

[b] η_{0lith} and η_{0um} are pre-exponential factors for the viscosity equation for the top 150 km and between 150 km and 670 km depths. η_0 for the lower mantle is 1.

[c] I.C. represents the initial conditions which are either random perturbation or perturbation at some given spherical harmonic degree l and order m, or from a temperature field of other calculation.

[d] ξ is the internal heating rate, and Q_s and V_s are representative mean surface heat flux and mean surface velocity that are dimensionalized using parameters in Table 1.

[e] Under column for structure, if the stable degree-1 platform with one downwelling and one upwelling is achieved, the latitude and longitude of the centroid of the single downwelling are given in the parentheses. Otherwise, the dominant harmonic degrees are given.

has a perturbation at spherical harmonic degree l=3 and order m=2. We compute the case for ~50,000 time-steps to a statistical steady state. The representative planform of mantle convection is characterized by relatively short-wavelength structure with a large number of evenly distributed upwellings and downwellings (Fig. 2a). Power spectra for temperature within the bottom thermal boundary layer display a maximum amplitude at degree 6 (Fig. 3a). The horizontally averaged viscosity shows a relatively strong lithosphere due to temperature-dependent viscosity (Fig. 3b). Internal heating rate computed by time-averaging surface and bottom heat flux is ~50% (Table 2).

Case 2 differs from Case 1 only in having a reduced upper mantle and lithospheric viscosity with $\eta_0(r)$=1/30 and 1 above and below the 670 km depth, respectively (Table 2). Such a distribution in $\eta_0(r)$ is similar to that in Bunge et al. (1996). However, Bunge et al. (1996) did not consider temperature-dependent viscosity. For Case 2 in a statistical steady state, internal heating rate is ~44% (Table 2), and the representative thermal structure is again characterized by relatively short wavelengths (Figs. 2b and 3a). Compared with Case 1, Case 2 has even shorter characteristic wavelengths in its thermal structure. This indicates that a viscosity increase at the 670 km depth may not necessarily lead to an increase in structural wavelengths, suggesting an important role of temperature-dependent viscosity.

Case 3 differs from Case 1 only in having a reduced upper mantle viscosity with $\eta_0(r)$=1/30 between 150 km and 670 km depths and $\eta_0(r)$=1 elsewhere (Table 2). Compared with Case 2, Case 3 has a stronger lithosphere. The planform of mantle convection for Case 3 (Figs. 2c, d and 3a) has much longer wavelengths than either Cases 1 or 2. The final, stable flow structure is now predominantly degree-1 in that one hemisphere is occupied by one major upwelling while the other by one downwelling (Figs. 2d and 3a). The single downwelling in the final degree-1 planform in Fig. 2d grows from one dominant downwelling that absorbs other three smaller downwellings (Fig. 2c). The surface heat flux increases during the structural transition to the degree-1 planform (Figs. 4a and b), mainly due to increased convective motion, as evident in the surface motion (Fig. 4a). The internal heating rate for Case 3 is ~40% (Table 2). Note that the nondimensional times for the snapshots in Fig. 2c and d are 0.00167 and 0.00278, respectively (Figs. 4a and b).

Cases 4 and 5 differ from Case 3 only in initial conditions with random initial perturbation for Case 4 and l=6 and m=4 for Case 5 (Table 2). Notice that in Case 5 with l=6, the perturbation is symmetric about the equator of numerical grids. For both cases, the final, stable convective structure shows a degree-1 planform that is nearly identical to that for Case 3 (Fig. 2d) but with the single downwelling centered at different locations (Table 2). A degree-1

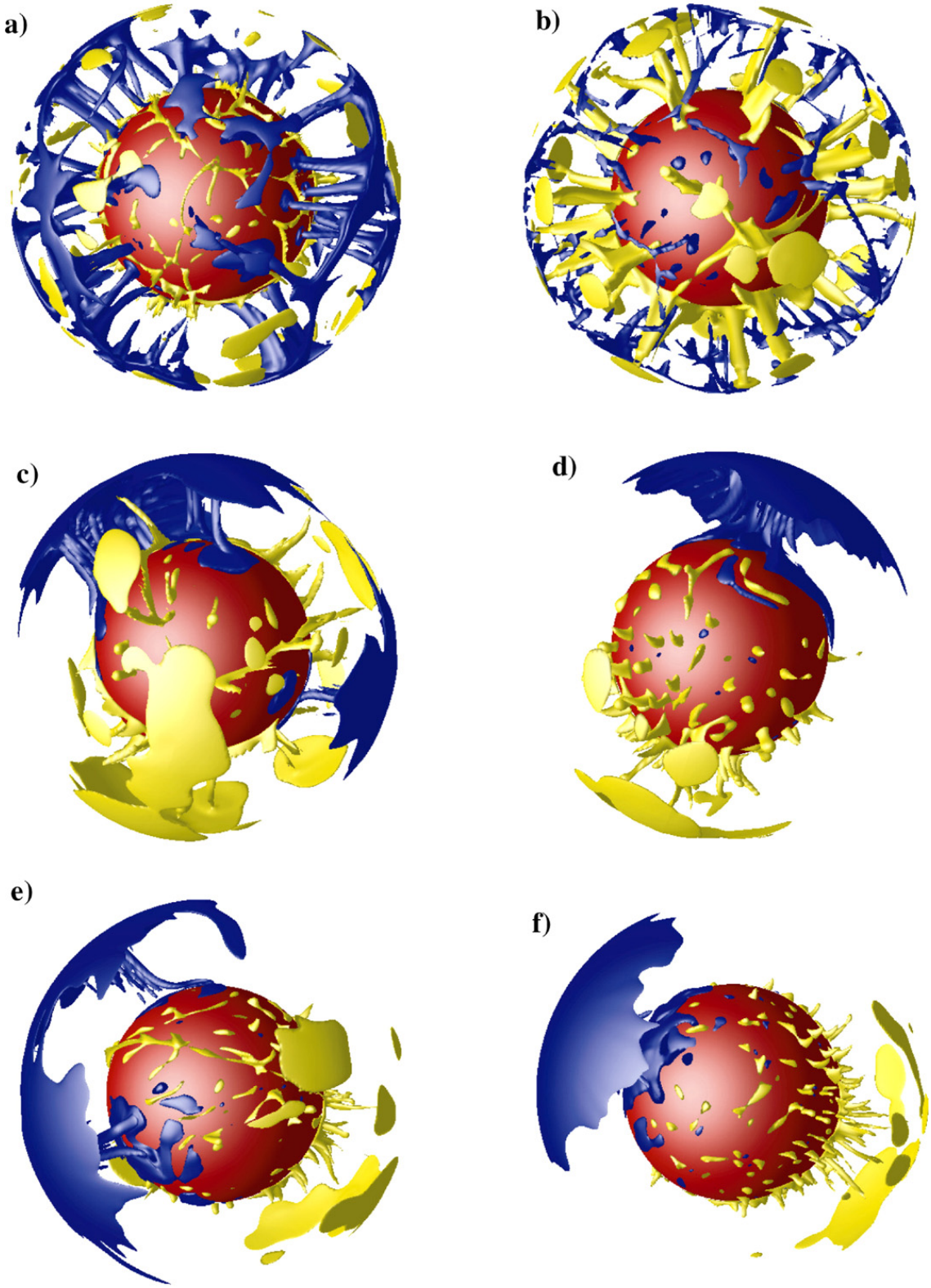

Fig. 2. Representative thermal structures for Cases 1 (a), 2 (b), Case 3's early stage of a degree-1 planform (c) and stable degree-1 planform (d), and Case 9's early stage of a degree-1 planform (e) and stable degree-1 planform (f). Thermal structures are plotted as isosurfaces of residual temperature $T-\overline{T}(r)$ with contour levels of -0.15 (blue for relatively cold mantle) and 0.15 (yellow for relatively hot mantle). The plots are orientated to best illustrate characteristic features in thermal structure, but (c) and (d) have the same orientation and so do (e) and (f).

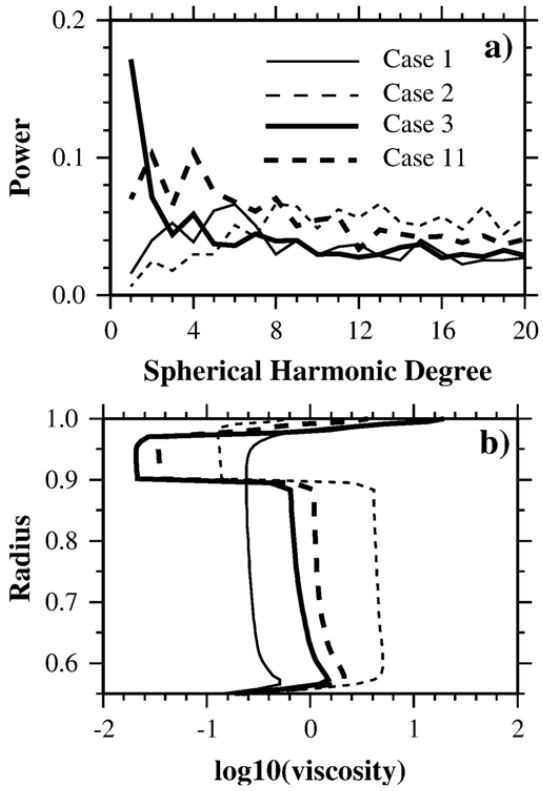

Fig. 3. The representative power spectrum of the bottom thermal boundary layer (a) and depth dependence of horizontally averaged mantle viscosity (b) Cases 1, 2, 3 and 11. (a) and (b) have the same line convention which is given in Figure 3a. The results for Cases 1, 2 and 3 are for thermal structures given in Figs. 2a, b and c, respectively.

planform of mantle convection was also obtained in a calculation (not presented here) that employed the temperature from Case 1 in Fig. 2a as initial condition and used the same viscosity structure as in Case 3.

Additional cases with different Ra and γ also produce a degree-1 planform of mantle convection. These include Case 6 that differs from Case 3 only in that $\gamma=26.3$, Cases 7 and 8 that differ from Case 3 only in that $Ra=1.37\times10^6$ and 1.37×10^7, respectively, and Case 9 that has $Ra=1.37\times10^7$ but $\gamma=20.2$ (Table 2). For these cases, internal heating rate ranges from 29% to 61%, and Ra varies by more than one order of magnitude. Convective vigor in Cases 8 and 9 is close to that of the present-day mantle with averaged surface velocity of ~6 cm/year and heat flux of ~60 mW/m^2 (Table 2). Note that velocity and heat flux are scaled with κ/R and $k\Delta T/R$, respectively (Zhong et al., 2000), where the parameters are given in Table 1.

Although Cases 3–9 all reach a stable degree-1 planform with a single downwelling, the evolution of convection planform varies. Different from Case 3 in which the single downwelling grows from one dominant downwelling that absorbs other three smaller downwellings (Figs. 2c and d), in Case 9, the downwelling hemisphere has two downwellings of similar sizes for some extended period (Fig. 2e) before they merge into one (Fig. 2f). The planform evolution for all these cases largely falls into either of these two types. For simplicity, we refer the planform evolution in Cases 3 and 9 as asymmetric and symmetric evolutions, respectively.

Cases 1–3 suggest that lithospheric viscosity, in addition to the viscosity increase at 670-km depth, has significant effects on the formation of long-wavelength structure, particularly the degree-1 planform. To further examine these effects, we compute two additional cases, Cases 10 and 11 in which different from Case 3, $\eta_0(r)$ for the top 150 km of the mantle is reduced to 0.4 and 0.2, respectively, but is still larger than 1/30 for Case 2 (Table 2). While Case 10 shows essentially the same degree-1 planform as in Case 3, Case 11 displays

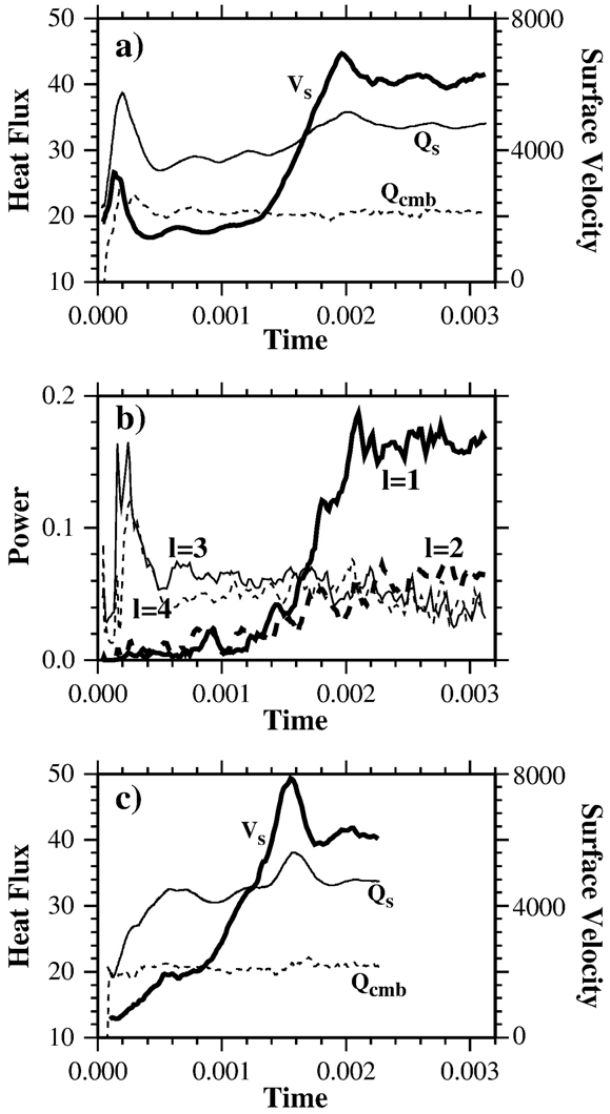

Fig. 4. The time-dependent averaged surface heat flux, Q_s, CMB heat flux, Q_{cmb}, and surface velocity, V_s (a), the power spectra of the bottom thermal boundary layer at degrees 1, 2, 3 and 4 (b) for Case 3, and time-dependent averaged Q_s, Q_{cmb} and V_s for Case 4 (c).

structures primarily at degrees 2 and 4 (Fig. 3a). For these cases producing a degree-1 planform, the averaged lithospheric viscosity is ~100–300 times of upper mantle viscosity. Such a lithospheric viscosity is generally consistent with that inferred from lithospheric deformation (England and Molnar, 1997).

Our results show that mobile-lid mantle convection with a relatively strong lithosphere and lower mantle is expected to have a degree-1 planform. These models do not include continents, and they should be applicable when continents are scattered around the Earth's surface with relatively small sizes. Continents with small sizes may not affect the global mantle flow significantly (Zhong and Gurnis, 1993). We think that such a degree-1 planform is responsible for supercontinent assembly with continents converging in the downwelling hemisphere, as suggested in previous kinematic models (Monin, 1991; Evans, 2003).

3.2. Effects of a supercontinent on planform of mantle convection

To understand supercontinent cycles, we must examine the effects of a supercontinent on the mantle (Zhong and Gurnis, 1993; Lowman and Jarvis, 1996; Lowman and Jarvis, 1995; Phillips and Bunge, 2005). Continental blocks with relatively large sizes, may collide to form a supercontinent in the downwelling hemisphere before the stable degree-1 planform with one downwelling such as in Fig. 2d is reached. However, for simplicity, our models with a supercontinent are started from the stable degree-1 planform of the preceding models but with a supercontinent placed above the single downwelling. The goal is to investigate the influence of a supercontinent on subsequent evolution of a degree-1 planform of mantle convection, assuming that the degree-1 planform causes the assembly of a supercontinent.

Three cases with a supercontinent based on Cases 3, 6 and 9 are computed. For these calculations, the longitude and latitude for the center of the downwelling from the degree-1 planform for each of Cases 3, 6 and 9 are determined first (Table 2). A supercontinent is then incorporated by centering it directly above the center of the downwelling. The temperature field from the degree-1 planform (e.g., Fig. 2d) is used as initial conditions for the calculation with a supercontinent. Since the basic results for these three cases with a supercontinent are similar, here we only present Case 3A which is a continuation of Case 3.

For Case 3A, as circum-supercontinent subduction starts, it drives return flow beneath the supercontinent that quickly replaces the initial downwelling with a hot upwelling in ~1.0 transit time (Fig. 5a). Transit time is

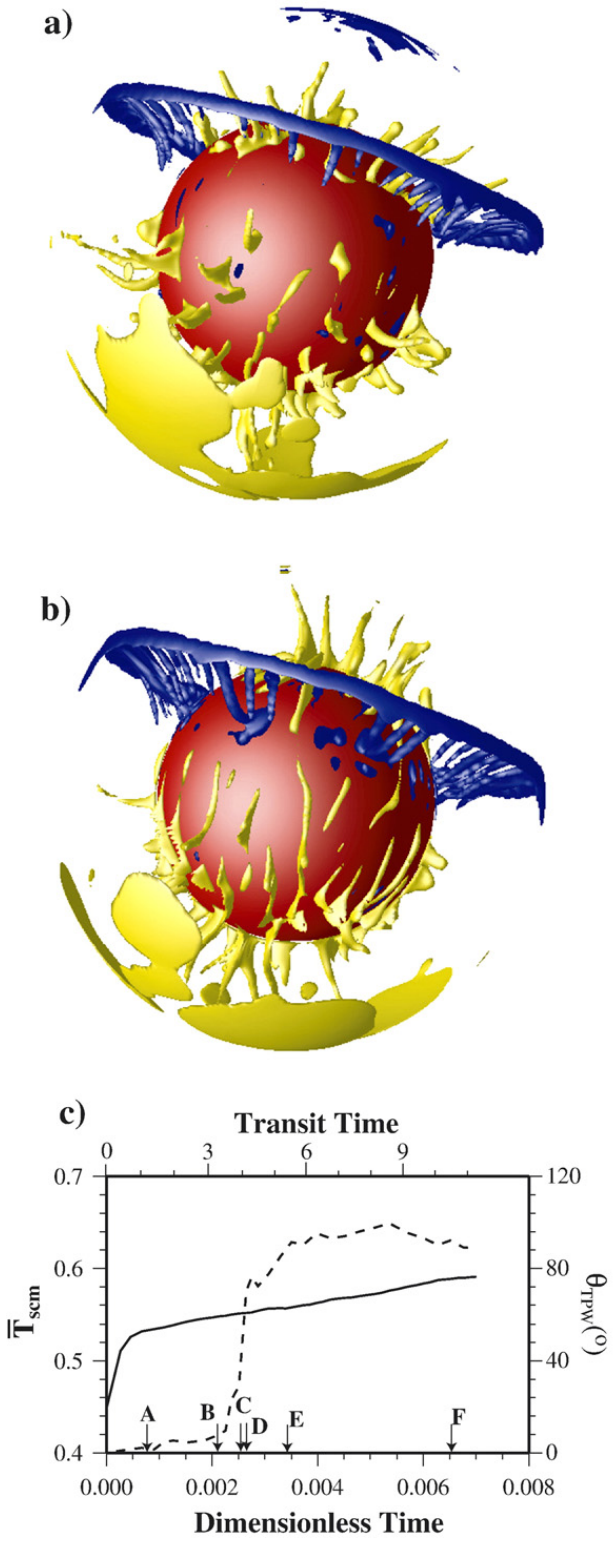

Fig. 5. Thermal structure for Case 3A with a supercontinent at ~one transit time (a) and five transit times (b) after the calculation starts (marked as A and E in (c), respectively), and time-dependence of subcontinental mantle temperature, $\overline{T}_{scm}$ (solid line) and TPW with respect to the initial pole position (dashed line) for Case 3A (c). $\overline{T}_{scm}$ is averaged over a region of the mantle below the supercontinent within a 30° arc distance to the center of the supercontinent.

defined as the time it takes for a fluid particle to travel from the surface to the core–mantle boundary at horizontally averaged flow speed at the surface (Zhong and Gurnis, 1993). One transit time for the Earth is ~50 Ma, if the averaged surface plate motion is taken as 6 cm/year. The two antipodal upwellings transform the initial degree-1 planform to degree-2 planform (Fig. 5b). During the first transit time, the averaged sub-continental mantle temperature over a region with arc radius of 30° from the center of the supercontinent, T_{scm}, increases at a dimensionless rate of $dT_{scm}/dt \sim 80$ (Fig. 5c), significantly larger than internal heating $\gamma = 10.1$, suggesting the upwelling as the cause for the temperature increase. T_{scm} continues to increase afterwards but at a much slower rate of $dT_{scm}/dt \sim 9$, which is comparable to γ, suggesting that the increase now is caused by internal heating and supercontinent's thermal insulation. The newly developed upwelling plumes beneath the supercontinent may eventually lead to volcanisms, rifting and breakup of the supercontinent (Gurnis, 1988).

3.3. TPW

The degree-1 planform that may cause supercontinent assembly, and degree-2 planform that is caused by a supercontinent represent a significant change in mantle structure associated with supercontinent cycles. Such a change in long-wavelength mantle structure may affect the Earth's moment of inertia and rotational stability and cause TPW. We now examine the relationship between long-wavelength mantle convection, supercontinent cycles, and rotational stability (i.e., TPW) predicted from our models.

TPW occurs to place the negative long-wavelength (i.e., degree-2) geoid at the poles and the positive at the equator (Goldreich and Toomre, 1969; Steinberger and O'Connell, 1997; Richards et al., 1997). Because the geoid anomalies by definition exclude degree-1 components, during supercontinent assembly with largely degree-1 planform convection, the geoid is sensitive to secondary features of the mantle flow. For the stable degree-1 planform (e.g., Fig. 2d), the geoid is negative above both the upwelling and downwelling with the predicted rotational axis going through the centers of the downwelling and upwelling (Fig. 6a for Case 3). However, prior to this stable planform, the pole position is variable for different cases. For example, for cases with asymmetric downwelling growth such as in Case 3 where the single downwelling in the degree-1 planform grows out from a dominant downwelling absorbing smaller

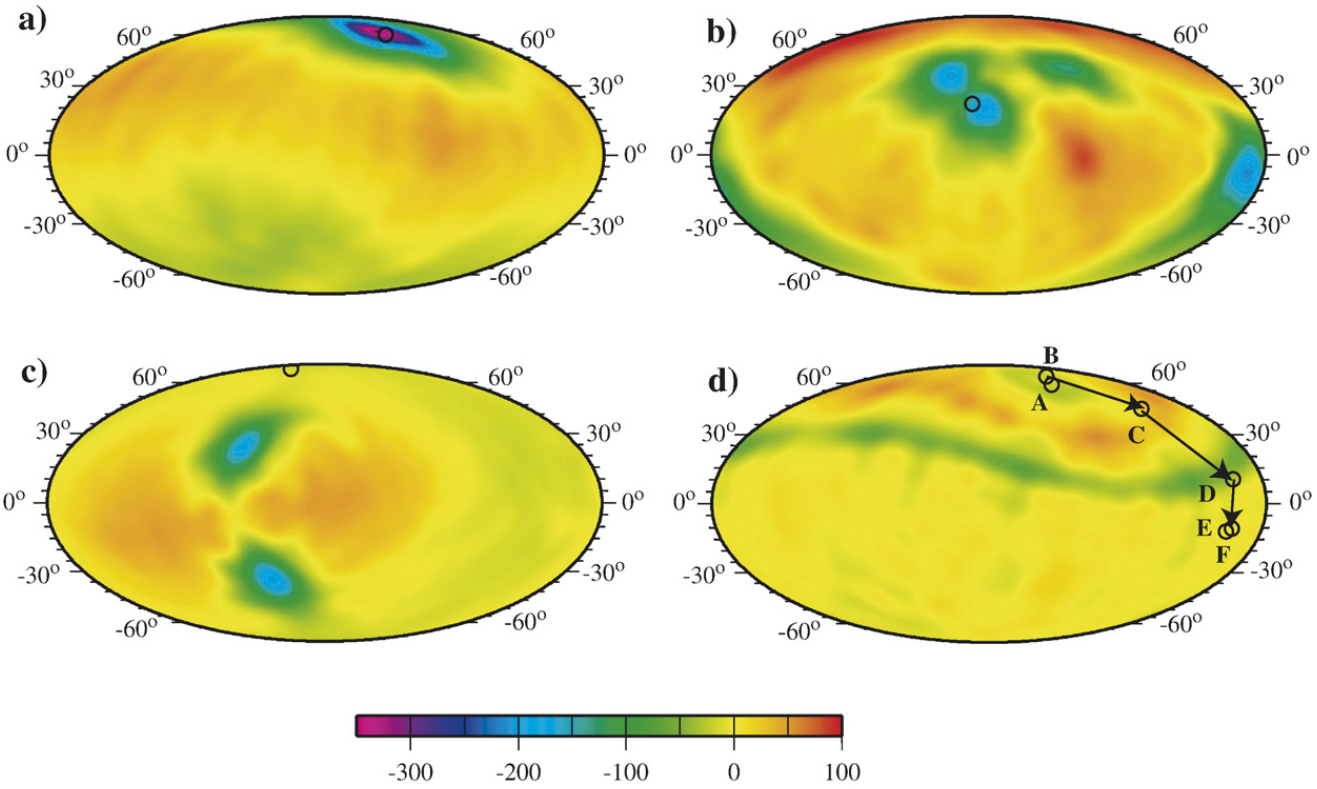

Fig. 6. The geoid and predicted rotational pole positions (black circle) for Case 3 with thermal structures in Figs. 2d (a) and c (b), for Case 9 with thermal structure in Fig. 2e (c), and for Case 3A with thermal structure in Fig. 5b at time E marked in Fig. 5c (d). In (d), pole positions at 6 different times as marked in Fig. 5c are also plotted to show the polar wander path. The geoid in meters is scaled using the parameters in Tables 1 and 2.

downwellings, the predicted pole stays near the center of the dominant downwelling, but migrates with time (Figs. 6a and b for Case 3). However, for Case 9 with symmetric downwelling growth (Figs. 2e and f), the geoid is positive between the two downwellings and the predicted pole is such that the equator runs between the two downwellings (Fig. 6c), differing greatly from cases with asymmetric downwelling growth (Fig. 6b). This suggests that a supercontinent may form near the pole for asymmetric downwelling growth cases (e.g., Case 3) or near the equator for symmetric growth cases (e.g., Case 9), assuming that for the latter scenario continental blocks are sufficiently large to form a supercontinent before the two downwellings merge.

We now examine the effect of a supercontinent on TPW. For Case 3A, initially and even after the sub-supercontinent upwelling is developed, the negative geoid and the pole are at the center of supercontinent, similar to those from the stable degree-1 planform in Case 3 (Fig. 6a). However, as T_{scm} increases and degree-2 structure strengthens, the geoid becomes positive above both upwellings including one below supercontinent (Fig. 6d), causing rapid TPW to place the two antipodal upwellings and the supercontinent at the equator and the poles at ~90° away (Figs. 5c and d). This suggests that after two antipodal upwellings are formed as a result of supercontinent assembly, the supercontinent is always expected to locate at the equator. This implies that if a supercontinent forms initially near a pole (e.g., for Case 3 with asymmetric downwelling growth), a subsequent large TPW is expected to place the supercontinent at the equator. However, if a supercontinent forms at the equator as it may in symmetric downwelling growth cases (e.g., Fig. 2e for Case 9), the supercontinent may remain at the equator as the sub-supercontinent upwelling and degree-2 structure develop.

4. Discussions

4.1. Very long-wavelength planform for mobile-lid convection

Our modelling results demonstrate that mantle convection with no continents is predominated by a degree-1 planform, provided that the viscosity of the upper mantle is ~100–300 times smaller than the viscosity of lithosphere and ~30 times smaller than that for the lower mantle. Such a viscosity structure for the mantle and lithosphere is consistent with observations of the long-wavelength geoid (Hager and Richards, 1989) and lithospheric deformation (England and Molnar, 1997). Our results indicate that a weak lithosphere promotes small-scale boundary layer instabilities and leads to reduced wavelengths of mantle convection. These results are insensitive to Rayleigh number (i.e., convective vigor) and internal heating rates for models that we have computed.

Our result that the combination of moderately strong lithosphere and lower mantle produces very long-wavelength mantle convection at high Rayleigh number differs significantly from that of previous studies (Bunge et al., 1996; McNamara and Zhong, 2005b; Harder, 2000; Yoshida and Kageyama, 2005). Bunge et al. (1996) showed in models with depth-dependent but not temperature-dependent viscosity that a viscosity increase of a factor of 30 from the upper to lower mantle may increase the long-wavelength convection that is predominated at spherical harmonic degree 6. However, their models used lithospheric viscosity that is the same as that for the upper mantle, which may be the reason that their models produced significantly shorter wavelengths than ours. Our results suggest that lithospheric viscosity plays an equally important role in controlling the planform of mantle convection as viscosity increase from the upper to lower mantles. In fact, our models with temperature- and depth-dependent viscosity indicate that the propensity of a viscosity increase at the 670-km depth for increasing convective wavelength can be completely offset by a weak lithosphere that promotes short-wavelength structures (comparing Cases 1 and 2, in Figs. 2a, b, and 3a). This indicates important effects of temperature-dependent viscosity on the planform of mantle convection.

A moderately strong lithosphere can lead to a degree-1 planform in spherical shell mantle convection without a viscosity increase from the upper to lower mantles (McNamara and Zhong, 2005b; Harder, 2000; Yoshida and Kageyama, 2005), but only for moderate convective vigor or Rayleigh number (McNamara and Zhong, 2005b). However, our results show that by combining the moderately strong lithosphere and a factor of 30 viscosity increase at the 670-km depth, the degree-1 planform is achieved with convective vigor that is comparable with that of the Earth (e.g., Case 9). In this study, we are mostly concerned with mobile-lid mantle convection which is more relevant to the Earth, and we did not attempt to increase the lithospheric viscosity to sufficiently large values to lead to stagnant-lid convection (Moresi and Solomatov, 1995). However, the degree-1 planform can also be obtained in stagnant-lid convection with sufficiently large viscosity increase at some mid-mantle depth (Roberts and Zhong, 2006).

It should be pointed out that as convective planform evolves from shorter wavelengths to a degree-1 structure, surface velocity increases significantly, and surface heat

flux also tends to increase (e.g., Figs. 4a and b for Case 3). Although such an increase in heat flux is less obvious or more like a transient phenomenon for some cases (e.g., Fig. 4c for Case 4), this may be consistent with the suggestion that a final, stable planform is such that the heat is released more efficiently (Lenardic et al., 2005).

4.2. Supercontinent cycles and very long-wavelength planform of convection

The degree-1 planform is generated from our models with no continent. We think that the results are applicable to the Earth with continental blocks scattered around the surface and moving passively along with global mantle flow without significant effects on global mantle flow. This assumption is supported by previous 2-D modelling studies (Zhong and Gurnis, 1993), but more modelling studies with multiple continental blocks are needed to further validate this assumption. We suggest that such a degree-1 planform is responsible for supercontinent assembly with the downwelling (upwelling) that pulls (pushes) all the continents towards the downwelling hemisphere. The time scale for forming a degree-1 planform in our models is moderately dependent on initial conditions and can be estimated in terms of transit times. For example, for Case 3, the characteristic non-dimensional surface velocity before a degree-1 planform is generated is ~ 1600 (Fig. 4a), and it takes non-dimensional time of $\sim 2\times 10^{-3}$ to reach the degree-1 planform (Fig. 4b) from an initial structure with perturbation at $l=3$ and $m=2$. That is, it takes ~ 7 transit times or ~ 350 Ma to generate a degree-1 planform, assuming that one transit time is ~ 50 Ma for the Earth. This 350 Ma time scale is consistent with the time scales for supercontinent cycles.

Our calculations also show that a supercontinent, once formed in the downwelling hemisphere, induces another upwelling system below the supercontinent, transforming the degree-1 planform that drives the supercontinent assembly to a largely degree-2 planform with two antipodal upwellings. Our calculations demonstrate that the sub-supercontinent upwelling plume (or superplume) is developed on a relatively short time-scale (~ 1 transit time or ~ 50 Ma), mainly as a result of a return flow in response to circum-supercontinent subduction. This is consistent with the relatively short period of time from completion of supercontinent assembly to continental volcanisms as observed for Pangea and Rodinia (Li et al., 2004; Li et al., in press; Smith et al., 1981). Thermal insulation from a supercontinent plays a minor role in developing the sub-supercontinent upwelling plume (Lowman and Jarvis, 1996; Lowman and Jarvis, 1995), although it may help further heat up the sub-supercontinent mantle. As suggested by Gurnis (1988) and observed for both Pangea and Rodinia (Li et al., 2003), the sub-supercontinent upwelling plume may lead to continental rifting, volcanisms and eventual breakup of the supercontinent. Although time scale from the formation of the sub-supercontinent plume to supercontinent breakup may depend on the rifting process, it is estimated to be ca. 100 Ma for both Rodinia and Pangea (Li et al., 2003).

We suggest that after the supercontinent is dispersed into small blocks that do not affect global mantle flow, the mantle should return to a degree-1 planform again, thus leading to assembly of another supercontinent and supercontinent cycles. This suggests that due to modulation of continents, the Earth's mantle convection oscillates between a degree-1 planform and a degree-2 planform. Such an evolutionary process leads to cyclic assembly and dispersal of supercontinent at the Earth's surface.

Our proposed scenario for mantle structure evolution has important implications for present-day mantle seismic structure. The present-day lower mantle structure is predominated by degree-2 structures with the Africa and Pacific superplumes surrounded by subduction (Dziewonski, 1984; Masters et al., 2000; Ritsema et al., 1999; Romanowicz and Gung, 2002; Van der Hilst, 1997; Grand, 2002) (Fig. 1c). Furthermore, the Africa superplume is approximately antipodal to the Pacific superplume and is located below the center of Pangea. This is consistent with our model prediction for the degree-2 planform of convection with two antipodal upwelling plumes that results from dynamic interaction between an initially degree-1 planform and a supercontinent. This suggests that the present-day long-wavelength structure in the lower mantle (i.e., the Africa and Pacific superplumes) is largely the same as that in the Pangea time, which may be expected considering that the present-day plate motion largely reflects a continuation of the breakup process of Pangea that started ~ 175 Ma ago (Smith et al., 1981; Scotese, 1997; Lithgow-Bertelloni and Richards, 1998; Anderson, 1982). This is also consistent with the recent suggestion based on surface volcanism that the locations of the Africa and Pacific superplumes have not changed significantly for at least the last 250 Ma since the eruption of the Siberian Traps (Torsvik et al., 2006). Our model further suggests that the Pacific superplume that drove the Pangea assembly should be significantly older than the Africa superplume which was formed after Pangea was assembled.

4.3. Supercontinent cycles and TPW

TPW occurs to place the negative degree-2 geoid at the poles and the positive at the equator (Goldreich and

Toomre, 1969; Steinberger and O'Connell, 1997; Richards et al., 1997). For the present-day Earth, the degree-2 positive geoid anomalies are over Africa and Pacific (antipodal) and are controlled by the lower mantle structures (Hager and Richards, 1989) including the Africa and Pacific upwellings and circum-Pacific subduction (Dziewonski, 1984; Masters et al., 2000; Ritsema et al., 1999; Van der Hilst, 1997; Grand, 2002) (Figs. 1c and d). The stability of these mantle structures may be responsible for relatively small TPW in the last 120 Ma (Steinberger and O'Connell, 1997; Richards et al., 1997). We now examine the implications of our models for TPW in supercontinent cycles.

An inference from these TPW calculations is the equatorial location of a supercontinent at its final stage. This is dictated by the positive geoid anomalies from the two antipodal upwellings (Figs. 5b and 6d). This result is consistent with Pangea and Rodinia's equatorial positions before their breakup (Fig. 1a and b). In contrast to Anderson (1982) who suggested that the Pangea's equatorial location results from two antipodal geoid highs caused by Pangea's insulation effects, we emphasize the role in producing antipodal geoid highs from two antipodal upwellings that naturally arise from supercontinent processes. The degree-2 structure with two major antipodal upwellings surrounded by subduction should be stable for some extended period after supercontinent breakup, as indicated by the present-day mantle structure as aftermath of Pangea's breakup. This suggests that the TPW should be relatively small after a supercontinent acquires its equatorial location and during the breakup, possibly until the supercontinent is fully dispersed and mantle convection starts to return to a degree-1 planform.

However, our model predicts that TPW is expected to be more variable and larger during supercontinent assembly and before a supercontinent acquires an equatorial location. This is because during supercontinent assembly, the degree-2 geoid anomalies that control the TPW are sensitive to more subtle secondary features of largely degree-1 mantle flow that drives the assembly. For example, thermal structures in Fig. 2c and 2e for Cases 3 and 9 both have a similarly strong degree-1 component but differ at shorter wavelengths. However, the predicted pole positions relative to the predominant downwelling are significantly different (Figs. 6b and c).

Indeed, the observations for Pangea and Rodinia seem to support this inference. After its formation, Rodinia may experience a large TPW to move it from the pole to equator (Li et al., 2004; Li et al., in press; Maloof et al., 2006). This is similar to that from Cases 3 and 3A with asymmetric downwelling growth in which the supercontinent is predicted to form near the pole but subsequently move to the equator due to TPW associated with the formation of second upwelling plume below the supercontinent (Figs. 2c, 6a, and 6d).

However, Pangea does not experience significant TPW after its two major building blocks, Gondwanaland and Laurussia, collide near the equator (Smith et al., 1981; Scotese, 1997; Evans, 2003), although large TPW was suggested for Gondwanaland (Van der Voo, 1994). For symmetric downwelling growth as in Case 9, two large continental blocks such as Gondwanaland and Laurussia may collide to form a supercontinent near the equator before two downwellings of similar strength in the downwelling hemisphere merge into a single downwelling (Fig. 2e and 6c). The subsequent development of sub-supercontinent upwelling plume may further stabilize the equatorial location of the supercontinent, as for Pangea.

5. Conclusions

Our results can be summarized as follows.

1 Mobile-lid mantle convection with observationally constrained mantle and lithospheric viscosities (i.e., moderately strong lithosphere and lower mantle, relative to the upper mantle) for a large range of Rayleigh number and internal heating rate is characterized by a degree-1 planform with one hemisphere predominated by downwellings and the other hemisphere by upwellings. We suggest that the degree-1 planform is responsible for supercontinent assembly with downwellings (upwellings) pulling (pushing) continental blocks to collide in the downwelling hemisphere.
2 A supercontinent, once formed in the downwelling hemisphere, induces another upwelling system below the supercontinent, transforming the degree-1 planform to largely degree-2 planform with two antipodal upwellings. This upwelling plume may lead to volcanism, continental rifting and breakup of the supercontinent.
3 We suggest that after the supercontinent is dispersed into small blocks, the mantle should return to a degree-1 planform again, thus leading to assembly of another supercontinent and supercontinent cycles. We further suggest that due to modulation of continents, mantle convection oscillates between degree-1 and degree-2 planforms.
4 The largely degree-2 structure with the Africa and Pacific superplumes for the present-day lower mantle is mainly generated at the Pangea time as a result of dynamic interaction between supercontinent Pangea and an initially degree-1 mantle convection which

with the Pacific superplume as the main upwelling system leads to the assembly of Pangea. While the Africa superplume may form after Pangea, the Pacific superplume should be significantly older.

5 A supercontinent should be located near the equator at its final stage due to the degree-2 geoid anomalies induced by two antipodal upwellings. This is consistent with the observations for Pangea and Rodinia. Relatively small TPW is expected after a supercontinent acquires its equatorial location and during its breakup process as the degree-2 structure persists until the supercontinent is fully dispersed and mantle structure starts to turn into a degree-1 planform again. However, TPW during supercontinent assembly with degree-1 planform mantle convection is expected to be more variable and large, because the degree-2 geoid which controls the TPW at this stage depends on subtle secondary features of mantle convection.

There are a number of potential drawbacks and assumptions that future studies should address. First, our models with mobile-lid convection of moderately temperature-dependent viscosity do not accurately account for plate tectonics at the Earth's surface. We assume that the length scale of plates is controlled by mantle convection. Although we think that our mobile-lid convection models capture the essence of the plate tectonic style of mantle convection (e.g., the energy transfer and subduction processes), future studies should consider highly nonlinear deformation processes for the lithosphere (Tackley, 2000; Bercovici, 2003) to validate this assumption. Second, our models include either no continent, or only a supercontinent. Future studies should incorporate multiple continental blocks (Gurnis, 1988) to investigate the dynamic interaction between continents and very long-wavelength mantle convection with special attention to different time scales of the relevant processes. Third, future studies also need to provide better understanding on the physics controlling long-wavelength planform of mantle convection including the role of radially stratified viscosity in promoting long-wavelength structure (Zhong and Zuber, 2001; Lenardic et al., 2005) and the control on asymmetric or symmetric downwelling growth in degree-1 planform mantle convection.

Acknowledgment

The authors wish to thank two anonymous reviewers for their helpful comments. This work is supported by the US National Science Foundation, the David and Lucile Packard Foundation, and ARC Discovery Project grants (DP0450020 and DP0770228). CIG is thanked for distributing the software CitcomS that is used in this study. This is TIGeR publication No. 68.

References

Anderson, D.L., 1982. Hotspots, polar wander, Mesozoic convection and the geoid. Nature 297, 391–393.

Bercovici, D., 2003. The generation of plate tectonics from mantle convection. Earth Planet. Sci. Lett. 205, 107–121.

Bunge, H.-P., Richards, M.A., Baumgardner, J.R., 1996. Effect of depth-dependent viscosity on the planform of mantle convection. Nature 379, 436–438.

Bunge, H.P., Richards, M.A., Lithgow-Bertelloni, C., Baumgardner, J.R., Grand, S.P., Romanowicz, B., 1998. Time scales and heterogeneous structure in geodynamic earth models. Science 280, 91–95.

Dalziel, I.W.D., 1991. Pacific margins of Laurentia and East Antarctica–Australia as a conjugate rift pair: evidence and implications for an Eocambrian supercontinent. Geology 19, 598–60.

Dziewonski, A.M., 1984. Mapping the lower mantle — determination of lateral heterogeneity in P-velocity up to degree and order-6. J. Geophys. Res. 89, 5929–5952.

England, P., Molnar, P., 1997. Active deformation of Asia: from kinematics to dynamics. Science 278, 647–650.

Evans, D.A.D., 2003. True polar wander and supercontinents. Tectonophysics 362, 303–320.

Goldreich, P., Toomre, A., 1969. Some remarks on polar wandering. J. Geophys. Res. 74, 2555–2567.

Grand, S.P., 2002. Mantle shear-wave tomography and the fate of subducted slabs. Phil. Trans. R. Soc. London Ser. A 360, 2475–2491.

Gurnis, M., 1988. Large-scale mantle convection and the aggregation and dispersal of supercontinents. Nature 332, 695–699.

Gurnis, M., 1989. A reassessment of the heat transport by variable viscosity convection with plates and lids. Geophys. Res. Lett. 16, 179–182.

Hager, B.H., Richards, M.A., 1989. Long-wavelength variations in Earth's geoid: physical models and dynamical implications. Philos. Trans. R. Soc. London, Ser. A 328, 309–327.

Harder, H., 2000. Mantle convection and the dynamic geoid of Mars. Geophys. Res. Lett. 27, 301–304.

Hoffman, P.F., 1991. Did the breakout of Laurentia turn Gondwanaland inside-out? Science 252, 1409–1412.

Jaupart, C., Parsons, B., 1985. Convective instabilities in a variable viscosity fluid cooled from above. Phys. Earth Planet. Inter. 39, 14–32.

King, S.D., Hager, B.H., 1990. The relationship between plate velocity and trench viscosity in Newtonian and power-law subduction calculations. Geophys. Res. Lett. 17, 2409–2412.

Lambeck, K., 1980. The Earth's Variable Rotation: Geophysical Causes and Consequences. Cambridge University Press. 458pp.

Lenardic, A., Richards, M.A., Busse, F.H., 2006. Depth-dependent rheology and the horizontal length scale of mantle convection. J. Geophys. Res. 111, B07404. doi:10.1029/2005JB003639.

Li, Z.X., Li, X.H., Kinny, P.D., Wang, J., Zhang, S., Zhou, H., 2003. Geochronology of Neoproterozoic syn-rift magmatism in the Yangtze Craton, South China and correlations with other continents: evidence for a mantle superplume that broke up Rodinia. Precambrian Res. 122, 85–109.

Li, Z.X., Evans, D.A.D., Zhang, S., 2004. A 90° Spin on Rodinia: possible causal links between the Neoproterozoic supercontinent, superplume, true polar wander and low latitude glaciation. Earth Planet. Sci. Lett. 220, 409–421.

Li, Z.X., Bogdanova, S.V., Collins, A.S., Davidson, A., De Waele, B., Ernst, R.E., Fitzsimons, I.C.W., Fuck, R.A., Gladkochub, D.P., Jacobs, J., Karlstrom, K.E., Lu, S., Natapov, L.M., Pease, V., Pisarevsky1, S.A., Thrane, K., Vernikovsky, V., in press. Assembly, configuration, and break-up history of Rodinia: a synthesis. Precamb. Res. doi:10.1016/j.precamres.2007.04.021.

Lithgow-Bertelloni, C., Richards, M.A., 1998. Dynamics of Cenozoic and Mesozoic plate motions. Rev. Geophys. 36, 27–78.

Lowman, J.P., Jarvis, G.T., 1995. Mantle convection models of continental collisions and breakup incorporating finite thickness plates. Phys. Earth Planet. Inter. 88, 53–68.

Lowman, J.P., Jarvis, G.T., 1996. Continental collisions in wide aspect ratio and high Rayleigh number two-dimensional mantle convection models. J. Geophys. Res. 101, 25,485–25,497.

Maloof, A.C., Halverson, G.P., Kirschvink, J.L., Schrag, D.P., Weiss, B.P., Hoffman, P.F., 2006. Combined paleomagnetic, isotopic, and stratigraphic evidence for true polar wander from the Neoproterozoic Akademikerbreen Group, Svalbard, Norway. GSA Bulletin 118, 1099–1124. doi:10.1130/B25892.1.

Masters, G., Laske, G., Bolton, H., Dziewonski, A., 2000. The relative behavior of shear velocity, bulk sound speed, and compressional velocity in the mantle: implications for chemical and thermal structure, in Earth's Deep Interior: Mineral Physics and Tomography From the Atomic to the Global Scale. In: Karato, S., et al. (Eds.), Geophys. Monogr. Ser., 117. AGU, Washington, D.C., pp. 63–87.

McNamara, A.K., Zhong, S., 2005a. Thermochemical structures beneath Africa and the Pacific Ocean. Nature 437, 1136–1139.

McNamara, A.K., Zhong, S., 2005b. Degree-1 mantle convection: dependence on internal heating and temperature-dependent rheology. Geophys. Res. Lett. 32, L01301. doi:10.1029/2004GL021082.

Monin, A.S., 1991. Planetary evolution and global tectonics. Tectonophysics 199, 149–1643.

Moores, E.M., 1991. Southwest U.S.–East Antarctic (SWEAT) connection: a hypothesis. Geology 19, 425–428.

Moresi, L., Gurnis, M., 1996. Constraints on the lateral strength of slabs from three-dimensional dynamic flow models. Earth Planet. Sci. Lett. 138, 15–28.

Moresi, L.N., Solomatov, V.S., 1995. Numerical investigation of 2D convection with extremely large viscosity variation. Phys. Fluids 9, 2154–2164.

Parmentier, E.M., Zhong, S., Zuber, M.T., 2002. Gravitational differentiation due to initial chemical stratification: origin of lunar asymmetry by the creep of dense KREEP. Earth Planet. Sci. Lett. 201, 473–480.

Phillips, B.R., Bunge, H.P., 2005. Heterogeneity and time dependence in 3D spherical mantle convection models with continental drift. Earth Planet. Sci. Lett. 233, 121–135.

Ricard, Y., Richards, M.A., Lithgow-Bertelloni, C., Le Stunff, Y., 1993. A geodynamic model of mantle density heterogeneity. J. Geophys. Res. 98, 21895–21909.

Richards, M.A., Ricard, Y., Lithgow-Bertelloni, C., Spada, G., Sabadini, R., 1997. An explanation for Earth's long-term rotational stability. Science 275, 372–375.

Ritsema, J., van Heijst, H.J., Woodhouse, J.H., 1999. Complex shear wave velocity structure imaged beneath Africa and Iceland. Science 286.

Roberts, J.H., Zhong, S., 2006. Degree-1 convection in the Martian mantle and the origin of the hemispheric dichotomy. J. Geophys. Res. 111, E06013. doi:10.1029/2005JE002668.

Roberts, J.H., Zhong, S., 2007. The cause for the north-south orientation of the crustal dichotomy and the equatorial location of Tharsis on Mars. Icarus 190, 24–31. doi:10.1016/j.icarus.2007.03.002.

Romanowicz, B., Gung, Y.C., 2002. Superplumes from the core–mantle boundary to the lithosphere: implications for heat flux. Science 296, 513–516.

Scotese, C.R., 1997. Continental Drift, 7th ed. PALEOMAP Project, Arlington, Texas. 79 pp.

Smith, A.G., Hurley, A.M., Briden, J.C., 1981. Phanerozoic Paleocontinental World Maps. Combridge Univ. Press.

Steinberger, B., O'Connell, R., 1997. Changes of the Earth's rotation axis owing to advection of mantle density heterogeneities. Nature 387, 169–173.

Tackley, P.J., 1996. Effects of strongly variable viscosity on three-dimensional compressible convection in planetary mantles. J. Geophys. Res. 101, 3311–3332.

Tackley, P.J., 2000. Self-consistent generation of tectonic plates in time-dependent, three-dimensional mantle convection simulations. 1. Pseudoplastic yielding. Geochem. Geophys. Geosyst. 1.

Torsvik, T., 2003. The Rodinia jigsaw puzzle. Science 300, 1379–1381.

Torsvik, T.H., Smethurst, M.A., Burke, K., Steinberger, B., 2006. Large igneous provinces generated from the margins of the large low-velocity provinces in the deep mantle. Geophys. J. Int. 167, 1447–1460.

van der Hilst, R.D., 1997. Evidence for deep mantle circulation from global tomography. Nature 386, 578–584.

van der Voo, R., 1994. True polar wander during the middle Paleozoic. Earth Planet. Sci. Lett. 122, 239–243.

Yoshida, M., Kageyama, A., 2006. Low-degree mantle convection with strongly temperature- and depth-dependent viscosity in a three-dimensional spherical shell. J. Geophys. Res. 111, B03412. doi:10.1029/2005JB003905.

Zhang, S., Yuen, D.A., 1995. The influences of lower mantle viscosity stratification on 3-D spherical-shell mantle convection. Earth Planet. Sci. Lett. 132, 157–166.

Zhong, S., Davies, G.F., 1999. Effects of plate and slab viscosities on geoid. Earth Planet. Sci. Lett. 170, 487–496.

Zhong, S., Gurnis, M., 1993. Dynamic feedback between an non-subducting raft and thermal convection. J. Geophys. Res. 98, 12219–12232.

Zhong, S., Zuber, M.T., 2001. Degree-1 mantle convection and Martian crustal dichotomy. Earth Planet. Sci. Lett. 189, 75–84.

Zhong, S., Zuber, M.T., Moresi, L.N., Gurnis, M., 2000. Role of temperature dependent viscosity and surface plates in spherical shell models of mantle convection. J. Geophys. Res. 105, 11063–11082.